

Dynamics of Entangled Polymers Confined between Graphene Oxide Sheets as Studied by Neutron Reflectivity

Ki-In Choi,^{†,‡} Tae-Ho Kim,[†] Guangcui Yuan,[§] Sushil K. Satija,[§] and Jaseung Koo^{*,†,‡}

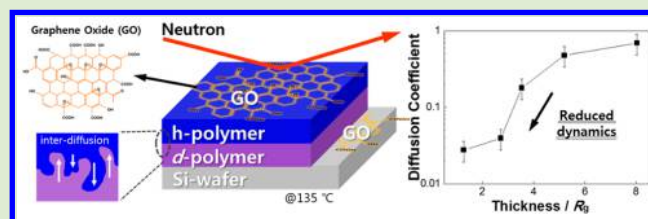
[†]Neutron Science Center, Korea Atomic Energy Research Institute (KAERI), Daejeon, 34057, Korea

[‡]Department of Organic Materials Engineering, Chungnam Nation University, Daejeon, 34134, Korea

[§]Center for Neutron Research, National Institute of Standards and Technology, Gaithersburg, Maryland 20899, United States

Supporting Information

ABSTRACT: For graphene-based composites, the dynamics of polymers confined between graphene sheets are a key parameter governing the overall mechanical properties of bulk materials. Here, we used neutron reflectivity (NR) to measure the diffusion dynamics of polymer melts confined between graphene oxide (GO) surfaces. From the NR results, we found that the diffusion coefficients of poly(methyl methacrylate) (PMMA) between the GO sheets were dramatically reduced by more than 1 order of magnitude when the film thickness was less than ~ 3 times the gyration radius of the bulk polymer (R_g), whereas the diffusion of the polystyrene (PS) films sandwiched between GO sheets was only three times slower as the PS thickness decreased from $\sim 8 R_g$ to $1 R_g$. This difference was due to the fact that the polymer-GO interaction significantly influences the dynamics of confined polymer melts.



Over the past decades, there has been an intense interest in polymer mobility in nanoconfinement systems.^{1–12} Polymer mobility varies considerably with film thickness, especially when the thickness is less than ~ 4 times the bulk radius of gyration of the polymers (R_g).⁷ Previous computer simulations and experimental studies have shown that polymer dynamics in confined systems are influenced by several complicated factors.^{2,5,13–15} For example, strongly attractive polymer–wall interactions form a dead layer (or glassy layer) of polymer near the solid walls, thereby reducing polymer mobility tremendously. Polymer dynamics are also decreased due to spatial confinement of polymer chains near the wall surfaces if the film thickness is close to the molecular size of the polymers. On the other hand, the reduced entanglement density of the polymer melt near the solid wall enhances polymer mobility under confinement.^{16–18} Due to these complicated factors, the origins of the different dynamics of confined systems are still not clear, although this is an important clue to elucidating the mechanism of enhanced mechanical properties in polymer nanocomposite systems.^{19–21} Depending on the interaction (attractive or repulsive), polymer segmental mobility around the nanoparticle can be hindered or enhanced, which also influences the glass transition temperature (T_g) of the polymer.²²

Recently, graphene-based polymer nanocomposites have been of particular interest due to the significant impact of graphene on polymer's physical properties.^{23–25} Graphene oxide (GO), obtained from chemical exfoliation of graphite, has been widely used for polymer nanocomposites due to good dispersion in aqueous solvents or polymer matrices,²³ and also its functionality as a compatibilizer in immiscible polymer blends.^{26,27} Simulation studies have predicted that GO sheets

reduce the mobility of poly(methyl methacrylate) (PMMA) films confined to them relative to bulk values without GO.²⁸ Near the GO surface, chain mobility is significantly restricted due to interactions of the polymer with the GO surface. However, to the best of our knowledge, experimental results of the dynamics of polymers confined between GO sheets have not been investigated, although the mobility of polymers confined at a molecular level plays a crucial role in the overall mechanical properties of bulk composite systems.^{19–21}

In this study, we prepared polymer thin films sandwiched between GO monolayers as a model composite system to provide a quantitative description, including the mobility reduction of polymers near GO surfaces. Two different cases of interaction were studied: (i) a strongly attractive interaction and (ii) a weakly attractive interaction of polymers with GO surfaces. A neutron reflectivity technique was used as a probe of confined polymer mobility sandwiched between GO monolayers. The diffusion dynamics as a function of polymer film thicknesses between GO monolayers can be directly compared with previous results of the mechanical properties of bulk systems with various concentration of the GO in the matrices.

Results and discussion: Bilayer films of PMMA/deuterated PMMA (*d*PMMA) and polystyrene (PS)/deuterated PS (*d*PS) sandwiched between GO monolayers (denoted as GO/PMMA/*d*PMMA/GO and GO/PS/*d*PS/GO, respectively), were prepared as illustrated in Figure 1a. The thickness (*d*) of each film in the bilayer was varied symmetrically from ~ 100

Received: June 8, 2017

Accepted: July 17, 2017

Published: July 19, 2017

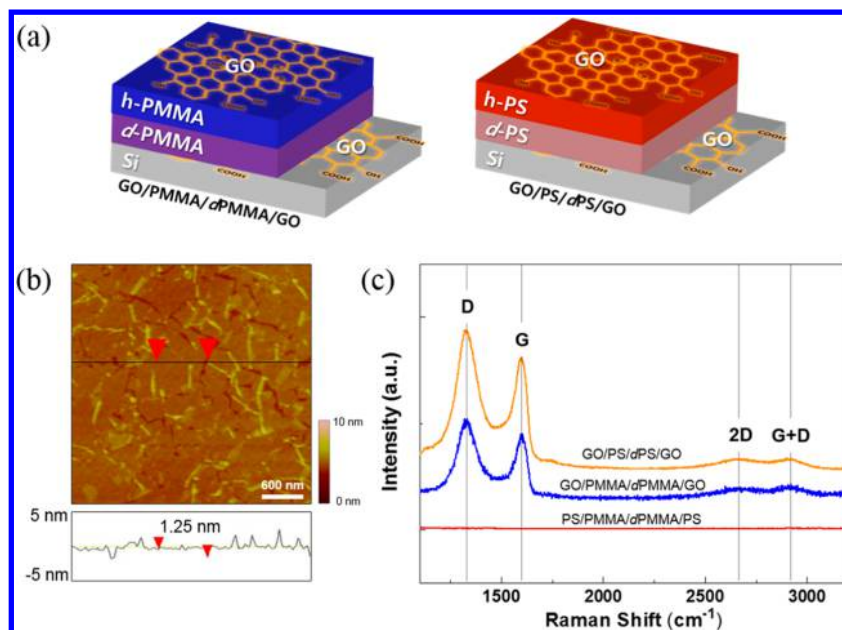


Figure 1. (a) Schematics of GO/PMMA/dPMMA/GO and GO/PS/dPS/GO; (b) AFM image of the GO monolayer transferred onto Si substrates by LS deposition; (c) Raman spectra of GO/PS/dPS/GO, GO/PMMA/dPMMA/GO, and PS/PMMA/dPMMA/PS.

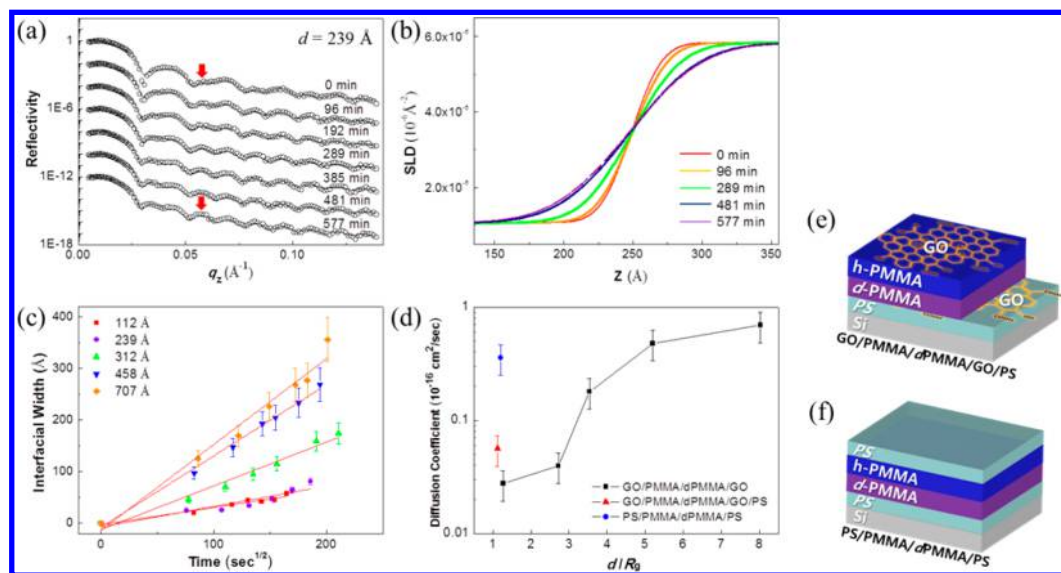


Figure 2. (a) Neutron reflectivity data of GO/PMMA/dPMMA/GO as a function of time, t , at 135 °C; (b) The corresponding SLD profile near the PMMA-dPMMA interface; (c) $\Delta\sigma$ plotted as a function of $t^{1/2}$; (d) D plotted as a function of the thickness, d ; (e) schematics of GO/PMMA/dPMMA/GO/PS; (f) schematics of PS/PMMA/dPMMA/PS.

to ~ 700 Å to investigate the effect of the GO surfaces on the diffusion dynamics of confined PMMA and PS thin films. GO is known to exhibit amphiphilic properties due to the hydrophobic basal carbon plane and the hydrophilic carboxylic group at the edges.²⁹ Therefore, PMMA can strongly interact with the oxidized domain of GO through hydrogen bonding, whereas PS has relatively weak interactions with the unoxidized basal plane through van der Waals forces and π - π stacking.²³ We measured contact angle (θ_c) of the PMMA and PS on the GO monolayers using AFM (Figure S1), where θ_c values were obtained to be 1.38° and 6.41°, respectively. This difference is due to stronger interaction between the PMMA and GO than that between the PS with GO. In this study, we thus investigated the role of the GO-polymer interaction on the

mobility of polymer chains in the thin films confined between GO sheets.

The GO monolayers were deposited using Langmuir-Schaefer (LS) and Langmuir-Blodgett (LB) techniques for the bottom and top layers of the GO monolayers, respectively, while the polymer layers were deposited by the floating technique (see Supporting Information for details).³⁰ The atomic force microscopy (AFM) results shown in Figure 1b revealed that the GO monolayers were densely packed upon the monolayer compression. The thickness of the GO layer was 1.25 nm, indicating a single layer.³¹ This close-packing morphology of the GO monolayer on the PMMA thin film was maintained even after annealing at 135 °C from the results of AFM (Figure S2) and neutron reflectivity (Figure S3). The presence of GO in the films was confirmed with Raman

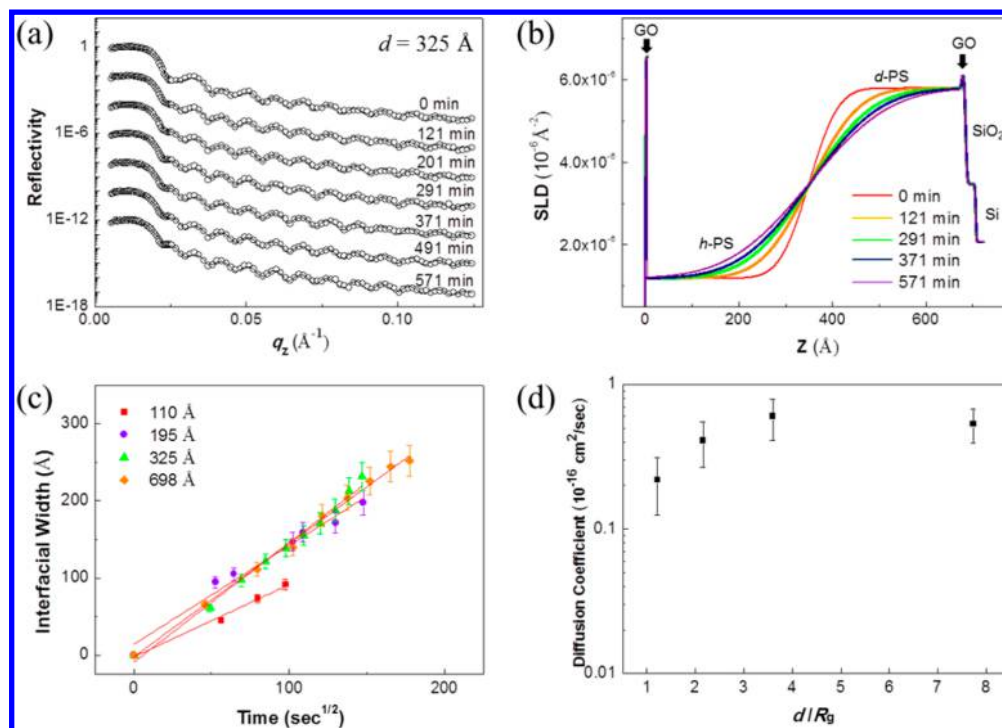


Figure 3. (a) Neutron reflectivity data of GO/PS/dPS/GO as a function of time, t , at 107 °C; (b) the corresponding SLD profile near the PS-dPS interface; (c) $\Delta\sigma$ plotted as a function of $t^{1/2}$; (d) D plotted as a function of the thickness, d . D of $\sim 8 R_g$ -thick sample is obtained to be 0.534×10^{-16} cm²/sec, which is consistent with D ($\sim 0.4 \times 10^{-16}$ cm²/sec) of PS ($M_w = 110$ kDa) using a forward-recoil spectrometry from a previous report.³⁸ Williams–Landel–Ferry (WLF) relationship was used to convert from D at 125 °C to D at 107 °C.

spectroscopy after deposition of the polymer films on the GO monolayers, as shown in Figure 1c. Typical peaks of GO sheets were obtained in the G, D, G+D, and 2D bands,³² indicating that the GO monolayers on the Si substrates were stable, without detachment, even after the deposition of the polymer layer by the floating technique. However, this feature of the Raman spectrum was not seen in the control PMMA/dPMMA bilayer confined between PS layers.

The structure of the GO-confined polymer thin films and their diffusion dynamics was measured by neutron reflectivity. Since the deuterated and nondeuterated polymers are chemically identical, neutron reflectivity results can provide the mobility information on the polymer chain itself from the variation in the concentration profiles across the interface between them as a function of annealing time. Figure 2a shows the typical neutron reflectivity profiles of GO/PMMA/dPMMA/GO ($M_w = 92$ and 110 kDa for PMMA and dPMMA, respectively) annealed at 135 °C as a function of time. The profiles in the low momentum transfer (q) region ($q < 0.07$ Å⁻¹) were significantly changed with time; new oscillation peaks appeared after annealing, as denoted with arrows, due to dPMMA-segmental diffusion to the PMMA layer. The scattering length density (SLD) profiles also show that the interface between the PMMA/dPMMA bilayer becomes broader with increasing time (Figure 2b). The broadening of the interface, $\Delta\sigma$, was corrected for the initial roughness, σ_0 . Thus, $\Delta\sigma$ is given by $\Delta\sigma = \sqrt{\sigma^2 - \sigma_0^2}$, where σ is the experimentally determined interfacial root-mean-square (rms) roughness. The values of $\Delta\sigma$ for the PMMA/dPMMA bilayer confined between GO monolayers with various film thicknesses were plotted as a function of time (Figure 2c). The rate at which the interface broadened, that is, the interdiffusion

rate, became significantly slower with decreasing the film thickness.

We obtained the diffusion coefficient (D) of the polymers from the interdiffusion rate and investigated the effect of the GO monolayers on the D values. From Figure 2c, we see that the interfacial width increases linearly with $t^{1/2}$; D is then extracted from the Fickian relationship, $\Delta\sigma = 2(Dt)^{1/2}$.³³ In Figure 2d, the D values are plotted as a function of d , showing that D approaches constant values (0.7×10^{-16} cm²/sec) for thicker samples ($d = \sim 5$ and $8 R_g$). This is in a good agreement with D of PMMA ($M_w = 120$ kDa) obtained using a forced Rayleigh scattering technique.³⁴ As the thickness decreases to $\sim 1 R_g$, D dramatically decreases by a factor of up to 25 ($D = 0.028 \times 10^{-16}$ cm²/sec). This indicates that the interaction between PMMA and the GO surface is strongly attractive, significantly suppressing the mobility of confined PMMA near the GO-polymer interface. This reduced diffusion is consistent with our previous report of dewetting dynamics, in which the dewetting hole of the PMMA thin films is completely prevented by the GO monolayer due to their attractive interactions.²⁶

It is known that the mobility of PMMA near the Si substrates significantly decreases due to the polymer pinning effect on the substrates. Hence, to eliminate the effect of attractive Si substrates on the diffusion dynamics of the GO-confined PMMA layer, we added spin-coated films of PS with high M_w (7100 kDa) between the bottom GO monolayer and Si surface, as illustrated in Figure 2e. GO/PMMA/dPMMA/GO with $d = \sim 1 R_g$ were prepared on PS substrates (denoted as GO/PMMA/dPMMA/GO/PS), and the neutron reflectivity was measured as a function of annealing time at the same temperature. We obtained that the diffusion coefficient values ($D = 0.056 \times 10^{-16}$ cm²/sec) were significantly low, similar to that for GO/PMMA/dPMMA/GO with $d = \sim 1 R_g$. This

indicates that the reduced dynamics were due to the PMMA-GO interaction rather than the PMMA-Si substrate interaction. For the sample in the absence of GO, that is, the PMMA/*d*PMMA bilayer sandwiched between the PS layers (denoted as PS/PMMA/*d*PMMA/PS and illustrated in Figure 2f) with $d \sim 1 R_g$, the diffusion coefficient was found to be 0.357×10^{-16} cm²/sec, which was 13-fold higher than the corresponding sample with GO.

This change in the diffusion dynamics due to the GO-PMMA interaction can be compared with the mechanical properties of bulk systems. For example, Brinson et al. reported that T_g was improved by nearly 30 °C by embedding 1 wt % of GO in the PMMA.³⁵ The rheological results of the GO-PMMA nanocomposites also have shown that zero shear viscosity (η_0) values determined by initial Newtonian plateau of viscosity (η) from steady shear experiments increased after adding 0.6 vol % (1.02 wt %) GO to the PMMA matrix.³⁶ From Einstein relationship, we compare this increase in η_0 with our diffusion results,

$$D = \frac{k_B T}{\eta_0 k_B / G(M) F(M, \nu)} \quad (1)$$

where $G(M)$ depends on the entanglement molecular weight and $F(M, \nu)$ is a function of the microstructural parameters of the polymer and k_B is Boltzmann constant.³⁷ Since D is inversely proportion to η_0 , the enhancement of viscosity of the bulk PMMA by the GO is due to the fact that diffusion dynamics of the PMMA is reduced by adding GO sheets.

In order to compare an interlayer spacing (l_g) of the GO sheets in the bulk composites with the thickness between the GO sheets for our systems, we calculated l_g from the simple equation, assuming a homogeneously dispersed layer structure formed by semi-infinite, parallel layers of GO sheets with thickness d_g . The interlayer spacing l_g varies with the volume fraction according to $\varphi = m/\varepsilon$, where m is the mass fraction and ε is the ratio of the densities of GO to polymer. One wt % of GO in the PMMA matrices corresponds to $l_g = 251$ Å, which is consistent with our results in which the diffusion coefficient began to decrease at nearly the same thickness of PMMA in the GO-sandwiched films. Therefore, we postulated that the previous results of mechanical improvement of the bulk GO-PMMA nanocomposites can be considered the cause of the reduced polymer diffusion dynamics confined between GO sheets in the matrices.

PS chains are also known to interact with the carbon basal plane in GO by van der Waals forces and π - π stacking.²³ However, this interaction is weaker than the GO-PMMA interaction.²³ Using neutron reflectivity, we also measured the diffusion dynamics of GO/PS/*d*PS/GO ($M_w = 106$ and 110 kDa for PS and *d*PS, respectively) with various film thicknesses (approximately $1 R_g < d < 8 R_g$) and measured the neutron reflectivity as a function of annealing time at 107 °C (Figure 3a). The SLD profiles show that as the annealing time increases, the interface between the PS layer and the *d*PS layer becomes broader, while the structure of GO layers remains unchanged regardless of annealing time. From the SLD profiles, we again plotted $\Delta\sigma$ as a function of annealing time to obtain the diffusion coefficient from the Fickian eq (Figure 3d). From this result, we found that the diffusion was reduced by only ~ 3 times as the polymer thickness decreased from approximately $8 R_g$ to $1 R_g$. This is significantly different from the dramatic reduction in diffusion seen in the GO/PMMA/*d*PMMA/GO

samples with a strong attractive interaction between GO and the polymers.

Previously, several groups have reported computational simulation studies on polymer structure and dynamics in confined polymer systems between solid walls using dynamic Monte Carlo (MC) and molecular dynamics (MD) methods.^{5,13,15,39} They investigated the effects of the interactions between the polymer–solid wall and the layer thickness of the polymers between the walls on the polymer conformation and diffusion dynamics. In the case of weak interactions between the polymer and wall, simulation results reveal that the relaxation time becomes only 2–3 times longer as the polymer film thickness decreases compared to that for the bulk polymers,⁵ which agrees with our diffusion results of GO/PS/*d*PS/GO. The weak interaction between the polymer-wall allows some chains to move from the surface to the middle of the polymer layers, whereas the strong interaction between the polymer–wall forms an immobile surface layer of adsorbed polymer chains like a glassy state.⁵ In our diffusion results, therefore, the reduction of diffusion dynamics of GO/PS/*d*PS/GO was not significant due to weaker attractive interaction compared to GO/PMMA/*d*PMMA/GO. We quantitatively measured the reduced D of polymer melts in confinement within GO sheets.

In summary, we used neutron reflectivity to study polymer mobility in thin films near graphene oxide (GO) surfaces. Model composite specimens were prepared, consisting of polymer thin films sandwiched between GO monolayers. In order to investigate the spatial confinement effect of the GO on the diffusion dynamics of polymer melts, a series of polymer PMMA/*d*PMMA or PS/*d*PS bilayers with various thicknesses confined between GO monolayers were prepared, and the neutron reflectivity measurements were performed as a function of annealing time at 135 °C. The results showed that diffusion coefficients of the PMMA in GO/PMMA/*d*PMMA/GO were dramatically reduced from 0.691×10^{-16} to 0.028×10^{-16} cm²/sec, whereas the diffusion of the PS in GO/PS/*d*PS/GO was suppressed by only three times from 0.534×10^{-16} to 0.219×10^{-16} cm²/sec when d decreases from $\sim 8 R_g$ to $1 R_g$. This difference is due to the degree of the attractive interaction between the GO and polymers.

■ ASSOCIATED CONTENT

Supporting Information

The Supporting Information is available free of charge on the ACS Publications website at DOI: 10.1021/acsmacrolett.7b00416.

Materials, sample preparation, and neutron reflectivity techniques (PDF).

■ AUTHOR INFORMATION

Corresponding Author

*E-mail: jkoo@kaeri.re.kr.

ORCID

Jaseung Koo: 0000-0002-3646-0805

Notes

The authors declare no competing financial interest.

■ ACKNOWLEDGMENTS

This work was supported primarily by a grant from by the National Research Foundation of Korea under Contract

2017M2A2A6A01019911. The identification of commercial products does not imply endorsement by the National Institute of Standards and Technology nor does it imply that these are the best for the purpose.

REFERENCES

- (1) Tree, D. R.; Wang, Y.; Dorfman, K. D. Mobility of a semi-flexible chain confined in a nanochannel. *Phys. Rev. Lett.* **2012**, *108*, 228105.
- (2) Yang, Z.; Fujii, Y.; Lee, F. K.; Lam, C.-H.; Tsui, O. K. C. Glass transition dynamics and surface layer mobility in unentangled polystyrene films. *Science* **2010**, *328*, 1676–1679.
- (3) Ok, S.; Steinhart, M.; Şerbescu, A.; Franz, C.; Chavez, F. V.; Saalwaechter, K. Confinement effects on chain dynamics and local chain order in entangled polymer melts. *Macromolecules* **2010**, *43*, 4429–4434.
- (4) Bansal, A.; Yang, H.; Li, C.; Cho, K.; Benicewicz, B. C.; Kumar, S. K.; Schadler, L. S. Quantitative equivalence between polymer nanocomposites and thin polymer films. *Nat. Mater.* **2005**, *4*, 693–698.
- (5) Aoyagi, T.; Takimoto, J.; Doi, M. Molecular dynamics study of polymer melt confined between walls. *J. Chem. Phys.* **2001**, *115*, 552–559.
- (6) Jones, R. The dynamics of thin polymer films. *Curr. Opin. Colloid Interface Sci.* **1999**, *4*, 153–158.
- (7) Lin, E. K.; Wu, W.-L.; Satija, S. K. Polymer interdiffusion near an attractive solid substrate. *Macromolecules* **1997**, *30*, 7224–7231.
- (8) Frank, B.; Gast, A. P.; Russell, T. P.; Brown, H. R.; Hawker, C. Polymer mobility in thin films. *Macromolecules* **1996**, *29*, 6531–6534.
- (9) Forrest, J. A.; Dalnoki-Veress, K.; Stevens, J. R.; Dutcher, J. R. Effect of free surfaces on the glass transition temperature of thin polymer films. *Phys. Rev. Lett.* **1996**, *77*, 2002–2005.
- (10) Bitsanis, I.; Hadziioannou, G. Molecular dynamics simulations of the structure and dynamics of confined polymer melts. *J. Chem. Phys.* **1990**, *92*, 3827–3847.
- (11) Kremer, K.; Binder, K. Dynamics of polymer chains confined into tubes: Scaling theory and Monte Carlo simulations. *J. Chem. Phys.* **1984**, *81*, 6381–6394.
- (12) Brochard, F.; de Gennes, P. G. Dynamics of confined polymer chains. *J. Chem. Phys.* **1977**, *67*, 52–56.
- (13) Li, S.; Li, J.; Ding, M.; Shi, T. Effects of polymer-wall interactions on entanglements and dynamics of confined polymer films. *J. Phys. Chem. B* **2017**, *121*, 1448–1454.
- (14) Hanakata, P. Z.; Douglas, J. F.; Starr, F. W. Interfacial mobility scale determines the scale of collective motion and relaxation rate in polymer films. *Nat. Commun.* **2014**, *5*, 4163.
- (15) Li, Y.; Wei, D.; Han, C. C.; Liao, Q. Dynamics of polymer melts confined by smooth walls: Crossover from nonentangled region to entangled region. *J. Chem. Phys.* **2007**, *126*, 204907.
- (16) Sussman, D. M.; Tung, W.-S.; Winey, K. I.; Schweizer, K. S.; Riggleman, R. A. Entanglement reduction and anisotropic chain and primitive path conformations in polymer melts under thin film and cylindrical confinement. *Macromolecules* **2014**, *47* (18), 6462–6472.
- (17) Tung, W.-S.; Composto, R. J.; Riggleman, R. A.; Winey, K. I. Local polymer dynamics and diffusion in cylindrical nanoconfinement. *Macromolecules* **2015**, *48*, 2324–2332.
- (18) Weir, M.; Johnson, D.; Boothroyd, S.; Savage, R.; Thompson, R.; King, S.; Rogers, S.; Coleman, K.; Clarke, N. Distortion of Chain Conformation and Reduced Entanglement in Polymer-Graphene Oxide Nanocomposites. *ACS Macro Lett.* **2016**, *5*, 430–434.
- (19) Lin, C.-C.; Parrish, E.; Composto, R. J. Macromolecule and particle dynamics in confined media. *Macromolecules* **2016**, *49*, 5755–5772.
- (20) Ganesan, V.; Jayaraman, A. Theory and simulation studies of effective interactions, phase behavior and morphology in polymer nanocomposites. *Soft Matter* **2014**, *10*, 13–38.
- (21) Karatrantos, A.; Composto, R. J.; Winey, K. I.; Kröger, M.; Clarke, N. Entanglements and dynamics of polymer melts near a SWCNT. *Macromolecules* **2012**, *45*, 7274–7281.
- (22) Ediger, M. D.; Forrest, J. A. Dynamics near free surfaces and the glass transition in thin polymer films: a view to the future. *Macromolecules* **2014**, *47*, 471–478.
- (23) Hu, K.; Kulkarni, D. D.; Choi, I.; Tsukruk, V. V. Graphene-polymer nanocomposites for structural and functional applications. *Prog. Polym. Sci.* **2014**, *39*, 1934–1972.
- (24) Ramanathan, T.; Abdala, A. A.; Stankovich, S.; Dikin, D. A.; Herrera-Alonso, M.; Piner, R. D.; Adamson, D. H.; Schniepp, H. C.; Chen, X.; Ruoff, R. S.; Nguyen, S. T.; Aksay, I. A.; Prud'Homme, R. K.; Brinson, L. C. Functionalized graphene sheets for polymer nanocomposites. *Nat. Nanotechnol.* **2008**, *3*, 327–331.
- (25) Stankovich, S.; Dikin, D. A.; Dommett, G. H. B.; Kohlhaas, K. M.; Zimney, E. J.; Stach, E. A.; Piner, R. D.; Nguyen, S. T.; Ruoff, R. S. Graphene-based composite materials. *Nature* **2006**, *442*, 282–286.
- (26) Kim, T.-H.; Kim, H.; Choi, K.-I.; Yoo, J.; Seo, Y.-S.; Lee, J.-S.; Koo, J. Graphene oxide monolayer as a compatibilizer at the polymer-polymer interface for stabilizing polymer bilayer films against dewetting. *Langmuir* **2016**, *32*, 12741–12748.
- (27) Cao, Y.; Zhang, J.; Feng, J.; Wu, P. Compatibilization of immiscible polymer blends using graphene oxide sheets. *ACS Nano* **2011**, *5*, 5920–5927.
- (28) Skountzos, E. N.; Anastassiou, A.; Mavrantzas, V. G.; Theodorou, D. N. Determination of the mechanical properties of a poly (methyl methacrylate) nanocomposite with functionalized graphene sheets through detailed atomistic simulations. *Macromolecules* **2014**, *47*, 8072–8088.
- (29) Li, D.; Müller, M. B.; Gilje, S.; Kaner, R. B.; Wallace, G. G. Processable aqueous dispersions of graphene nanosheets. *Nat. Nanotechnol.* **2008**, *3*, 101–105.
- (30) Kim, H.; Jang, Y. R.; Yoo, J.; Seo, Y.-S.; Kim, K.-Y.; Lee, J.-S.; Park, S.-D.; Kim, C.-J.; Koo, J. Morphology control of surfactant-assisted graphene oxide films at the liquid-gas interface. *Langmuir* **2014**, *30*, 2170–2177.
- (31) Cote, L. J.; Kim, F.; Huang, J. Langmuir-Blodgett assembly of graphite oxide single layers. *J. Am. Chem. Soc.* **2009**, *131*, 1043–1049.
- (32) Pimenta, M. A.; Dresselhaus, G.; Dresselhaus, M. S.; Cancado, L. G.; Jorio, A.; Saito, R. Studying disorder in graphite-based systems by Raman spectroscopy. *Phys. Chem. Chem. Phys.* **2007**, *9*, 1276–1290.
- (33) Doi, M.; Edwards, S. F. *The Theory of Polymer Dynamics*; Clarendon Press: Oxford, 1986.
- (34) Veniaminov, A. V.; Sillescu, H. Polymer and dye probe diffusion in poly (methyl methacrylate) below the glass transition studied by forced Rayleigh scattering. *Macromolecules* **1999**, *32*, 1828–1837.
- (35) Potts, J. R.; Lee, S. H.; Alam, T. M.; An, J.; Stoller, M. D.; Piner, R. D.; Ruoff, R. S. Thermomechanical properties of chemically modified graphene/poly (methyl methacrylate) composites made by in situ polymerization. *Carbon* **2011**, *49*, 2615–2623.
- (36) Vallés, C.; Young, R. J.; Lomax, D. J.; Kinloch, I. A. The rheological behaviour of concentrated dispersions of graphene oxide. *J. Mater. Sci.* **2014**, *49*, 6311–6320.
- (37) Green, P. F.; Kramer, E. J. Temperature dependence of tracer diffusion coefficients in polystyrene. *J. Mater. Res.* **1986**, *1*, 202–204.
- (38) Green, P. F.; Kramer, E. J. Matrix effects on the diffusion of long polymer chains. *Macromolecules* **1986**, *19*, 1108–1114.
- (39) Rissanou, A. N.; Harmandaris, V. Dynamics of various polymer-graphene interfacial systems through atomistic molecular dynamics simulations. *Soft Matter* **2014**, *10*, 2876–2888.